Kashani, M. (2017). Size Effect on Inelastic Buckling Behavior of Accelerated Pitted Corroded Bars in Porous Media. *Journal of Materials in Civil Engineering*, *29*(7), [1853]. https://doi.org/10.1061/(ASCE)MT.1943-5533.0001853

Size effect on inelastic buckling behaviour of accelerated pitted corroded bars in porous media

Mohammad M Kashani[1]

Abstract

A total of 110 inelastic buckling tests on corroded and uncorroded reinforcing bars with various bar diameters are conducted. Through regression analyses of experimental data the combined effect of nonuniform pitting corrosion and bar diameter (size effect) on buckling and post-yield buckling response of corroded and uncorroded bars are investigated. The experimental result shows that bar diameter has a minor influence on post-yield buckling response of uncorroded bars. However, it is found that bar diameter has a more significant impact on buckling capacity of corroded bars. Finally, the experimental data of tested corroded bars in this research are used to calibrate and update a new uniaxial material model of corroded bars to account for size effect. The proposed updated model simulates the inelastic buckling and post-buckling behaviour of corroded bars accounting for size effect. This model is implemented in an open source finite element code and is readily available to the community for nonlinear analysis of corroded reinforced concrete structures.

Keyword: Inelastic buckling, corrosion, reinforced concrete, constitutive model, stress-strain behaviour

[1]Lecturer, University of Bristol, Dept. of Civil Engineering University of Bristol, Bristol, BS8 1TR, United Kingdom (corresponding author), Email: mehdi.kashani@bristol.ac.uk

1. Introduction

Inelastic buckling of longitudinal reinforcing bars is the most common flexural failure mode of reinforced concrete (RC) components in major earthquakes (Lehman and Moehle 2000; Berry and Eberhard 2003; Kashani 2014). To this end, several researchers investigated the inelastic buckling behaviour of reinforcing bars experimentally and numerically using nonlinear finite element analysis technique (Bresler and Gilbert 1961; Bae et al. 2005; Cosenza and Prota 2006; Dhakal and Maekawa 2002; Mau and El-Mabsout 1989; Mau 1990; Monti and Nuti 1992; Pantazopoulou 1998; Papia and Russo 1989; Restrepo-Posada et al. 1994; Rodriguez et al 1999; Gomes and Appleton 1997).

Moreover, There is a large number of existing old RC structures and bridges in seismic regions that are also prone to chloride attack (deicing salt or sea water) (ASCE 2011). Therefore, these structures suffer from material deterioration and corrosion of reinforcing bars due to penetration of chloride ions. Accordingly, several researchers investigated the impact of corrosion on stress-strain behaviour of reinforcing bars (Almusallam 2001; Du et al. 2005a; Du et al. 2005b; Cairns et al. 2005; Apostolopoulos et al. 2006; Apostolopoulos 2007; Palssom and Mirza 2002).

Therefore, the combined effect of material ageing and earthquake hazard is one of the most important and popular topics among researchers in the recent years (Ghosh and Padgett 2010Alipour et al. 2011; Akiyama et al. 2011). Ou et al. (2013), Ma et al. (2012) and Meda et al. (2014) investigated the impact of corrosion on nonlinear behaviour of corroded RC components (beams and columns) experimentally. They have reported that corrosion has a significant impact on inelastic buckling of corroded RC components. More recently, Kashani et al. 2013a,b, Kashani et al. 2014 and Kashani et al. 2015a investigated the influence of corrosion on inelastic buckling of corroded reinforcing bars under monotonic and cyclic loading experimentally and numerically. The outcome of their research is development of a

48 novel nonlinear uniaxial material model (Kashani et al. 2015b) that is implemented in the
49 OpenSees (Openssees 2016) for nonlinear analysis of corroded and uncorroded RC structures
50 and bridges (Kashani et al. 2016a,b; Ni Chine et al. 2016).

51 In most of the previous studies of inelastic buckling behaviour of uncorroded and corroded
52 bars, researchers only investigated a single diameter reinforcing bars. Among those only
53 Monti and Nutti (1992) and Kunnath et al. (2009) reported that a change in bar diameter
54 might have an influence on inelastic buckling behaviour of uncorroded reinforcing bars. In
55 another study, Kashani et al. (2015c) reported that bar diameter might have a negative impact
56 on low-cycle fatigue life of uncorroded reinforcing bars but it doesn't affect the stress-strain
57 behaviour of these bars. However, there has not been any comprehensive experimental study
58 to explore the size effect on inelastic buckling and post-yield buckling behaviour of
59 uncorroded and corroded reinforcing bars. This is still an open issue to be addressed by
60 researchers.

61 The aim of this paper is to answer the following questions:

62 (i) Does bar diameter influence the buckling stress and post-yield buckling behaviour of
63 uncorroded bars?
64 (ii) Does bar diameter influence the significance of corrosion damage on inelastic buckling
65 of corroded bars?
66 (iii) Are the existing state-of-the-art computational (i.e OpenSees) and analytical (uniaxial
67 material models) models able to accurately simulate the post-yield buckling behaviour of
68 reinforcing bars with different bar diameters?

69 This paper is answering the above questions by exploring the influence of bar diameter on
70 inelastic buckling behaviour of uncorroded and corroded bars experimentally. A total of 110
71 buckling tests on uncorroded and corroded reinforcing bars are conducted. The test

specimens were varied in diameter and slenderness ratio. The impact of corrosion on maximum buckling stress (buckling capacity) and post-yield buckling behaviour of corroded bars with various diameters are investigated. Finally, a critical review on the accuracy of existing state-of-the-art computational and analytical models is provided and comparison between the experimental results and these models have been made.

The outcome of this study shows that bar diameter influences the post-yield buckling response of reinforcing bars with small slenderness ratio ($L/D \leq 8$, where L is the length and D is the diameter of bar). However as the slenderness ratio increases the influence of bar diameter on post-yield buckling response of uncorroded bars reduces. Although bar diameter influences the stress-strain behaviour of short uncorroded reinforcing bars (in post-buckling region), it is not significant enough to affect the inelastic behaviour of RC sections. In contrast, the experimental results show that bar diameter has a considerable negative impact on buckling stress loss (buckling capacity loss) of corroded bars. It is found that as bar diameter increases the influence of bar diameter on buckling of corroded bars also increases. The experimental results of this study are used to calibrate and update the new uniaxial material model developed by Kashani et al. (2015b).

2. Experimental programme

2.1 Specimen preparation

The corrosion of reinforcing bars inside concrete is a very slow process. Even in very aggressive environments it takes years for chloride ions to reach the reinforcement and initiate corrosion. Therefore, corrosion has to be realistically accelerated in the laboratory environment. To this end, a total of four reinforced concrete specimens were cast. Two specimens dimensioned 250×250×750mm incorporated 7 number 10mm diameter and 7 number 12mm diameter each cast, Further two specimens dimensioned 250×250×950mm were also cast that each of them incorporated 7 number 16mm diameter and 7 number 20mm

diameter reinforcing bars. The RC test specimens are shown in Fig. 1. The reinforcing bars used in this study were B500C British manufactured reinforcing bars (BS 4449 2005). The concrete mix was designed to have a mean compressive strength of 30MPa at 28 days with a maximum aggregate size of 12mm. The specimens were cast with a nominal cover of 25mm.

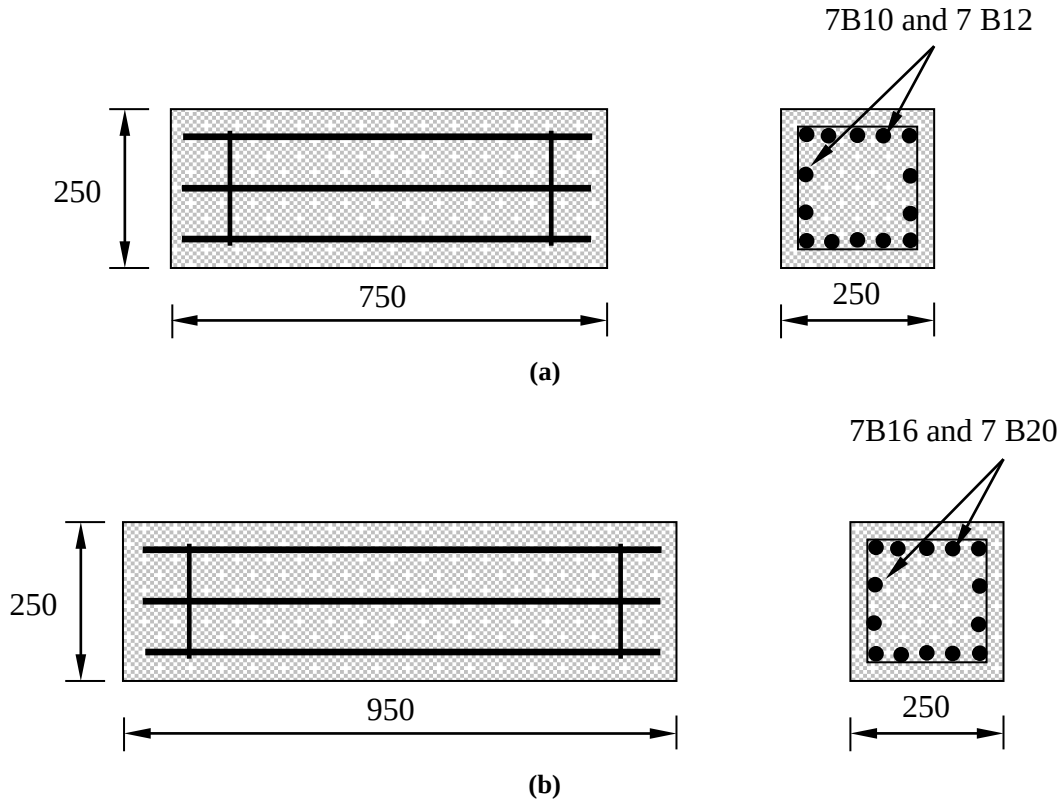

Fig. 1 Reinforced concrete specimens for accelerated corrosion

2.2 Corrosion simulation in the laboratory

An accelerated corrosion procedure (ACP) is employed to reduce the time required for reinforcing bars to reach the desired corrosion level. The ACP is a simple electrochemical circuit using an external power supply. In this circuit the reinforcing bars act as anode in the cell and an external material acts as cathode as shown in Fig. 2(a).

(a) **(b)**

Fig. 2 Accelerated corrosion procedure in the laboratory environment: (a) corrosion process in progress and (b) corroded specimen being demolished and corroded bars exposed

Faraday's 2nd Law of Electrolysis is employed to estimate the time required for desired corrosion level. After ACP, the corroded RC specimens were broken open carefully and the corroded bars were removed from the concrete. To clear the corrosion products and concrete from the surface of corroded reinforcement, a mechanical cleaning process using a bristle brush was used, in accordance with ASTM G1-03 (2011). The corroded bars were then washed with tap water and dried. The brushing and washing process was then repeated a second time. It should be noted that the same brushing process was applied to the uncorroded control specimens and it was found that the effect of brushing on the mass loss of base material is negligible. Further details of accelerated corrosion procedure and mass loss measurement method are available in Kashani et al. (2013a).

3. Experimental results and discussion

3.1 Tension tests and mechanical properties of uncorroded bars

The bar diameters considered in this research are 10mm, 12mm, 16mm and 20mm. For each group of test specimens three tension tests are conducted to characterise the mechanical properties of reinforcing bars. Table 1 summarises the mechanical properties of test

specimens (average value of three tension tests for each bar diameter) and Fig. 3 shows the typical stress-strain curve for each group of test specimens.

Table 1 Mechanical properties of tests specimens

Bar Diameter		**10mm**	**12mm**	**16mm**	**20mm**
Yield strain	ε_y	0.002686	0.002785	0.002733	0.002578
Yield stress (MPa)	σ_y	538	540	530	530
Elastic modulus (MPa)	E_s	200426	198501	193913	205603
Hardening strain	ε_{sh}	0.032310	0.03075	0.02547	0.023270
Strain at maximum stress	ε_u	0.152800	0.144800	0.164800	0.143600
Maximum stress (MPa)	σ_u	628	644	640	630
Fracture strain	ε_r	0.201800	0.215200	0.217350	0.217700

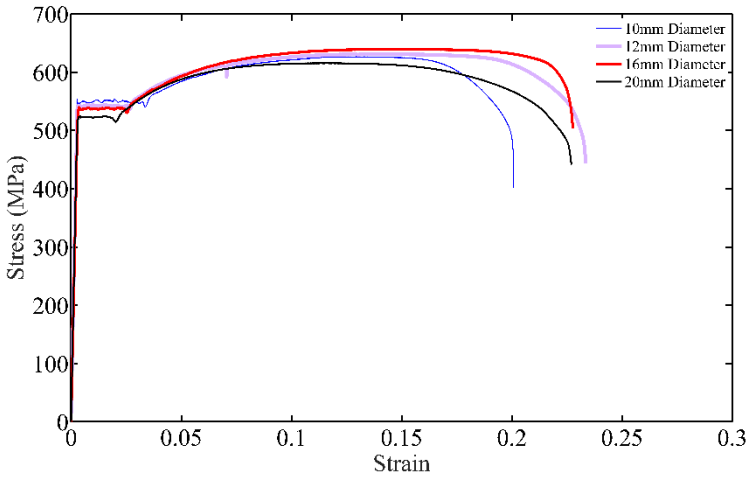

Fig. 3 Stress-strain behaviour of reinforcing bars in tension

3.2 Monotonic buckling experiment of uncorroded bars

A total of 24 monotonic buckling tests are conducted on uncorroded reinforcement with various effective lengths. The buckling lengths of bars are chosen based on the ratio of spacing of horizontal ties (L) in the common construction of RC columns to the bar diameter (D) known as the L/D ratio. The L/D ratios used in buckling tests of uncorroded bars are 5, 8, 10, 12, 15 and 20. A 250kN universal testing machine with hydraulic grips is used for the compression tests of the reinforcing bars. The machine incorporated an internal LVDT (linear Variable Differential Transducer) to measure the displacement of the grips. A 50mm extensometer with maximum stroke of ±5mm was used to measure the average axial strain over the middle section of the reinforcement over the linear range. An additional external

147 LVDT with maximum stroke of ±10mm was connected to the grips to measure the average
148 displacement over the entire length of the bar, in both linear and non-linear test phases.
149 Further details of the buckling experiment procedure are available in Kashani et al. (2013a).

150 Fig. 4 shows the results of buckling tests of uncorroded bars. The graphs in Fig. 4 are the
151 stress versus average strain over the entire length of the bar and therefore it is labelled *Mean*
152 *Strain* in Fig. 4. It should be noted that in Fig. 4(f) there is no experimental data presented for
153 20mm diameter bars. This is because the required length for L/D = 20 for 20mm diameter
154 bars was longer than the maximum stroke of the testing machine. Therefore it couldn't be
155 tested. Fig. 4(a) shows that the stress-strain response of the group of bars with L/D = 5 is very
156 similar to tension envelope. However, as the L/D increases the post-yield softening response
157 due to buckling is seen. Fig. 4(b) shows that the group of bars with L/D = 8 experience some
158 yield plateau before softening due significant lateral deformation induced by buckling. Fig. 4
159 shows that all of the bars with L/D > 8 have softening response immediately after yield stress.
160 Fig. 4 shows that the influence of bar diameter (size effect) is more significant in the group of
161 bars with L/D = 5 and 8. This is because in bars with small slenderness ratio ($L/D \leq 8$) the
162 spread of plasticity covers a significant portion of the entire length of the bar. Therefore, the
163 plasticity around the jaws (inelasticity around the boundary support), ribs pattern and size
164 effect at micro structure of material is more visible in the average stress-strain response.
165 However, in group of bars with L/D > 8 the spread of plasticity is localised (plastic hinges) in
166 three locations (both ends and in the middle). Therefore, the second order effect (geometrical
167 nonlinearity) has more significant influence on the stress-strain response than the size effect.
168 To investigate this phenomenon in more detail a 3D nonlinear continuum finite element
169 model should be employed. However, in structural engineering community, researchers and
170 engineers are interested in understanding and modelling the impact of stress-strain behaviour
171 of reinforcing bars on nonlinear response of RC section, components and structural systems.

Therefore, the change in post-yield buckling response of bars with $L/D \leq 8$ is not significant enough to affect the nonlinear response of RC sections and component. To this end, the impact of inelastic buckling is more significant than the size effect. In other words the difference in stress-strain behaviour of short bars ($L/D \leq 8$) caused by size effect (bar diameter) is negligible.

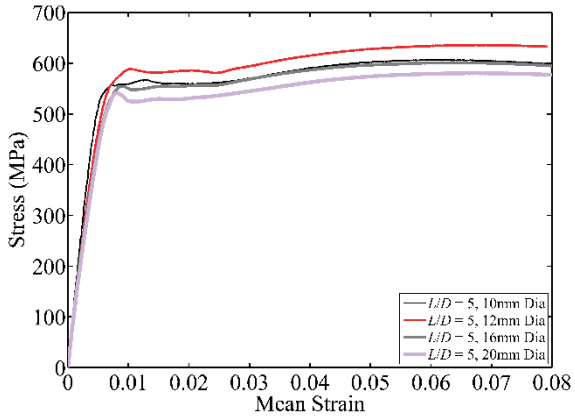

(a)

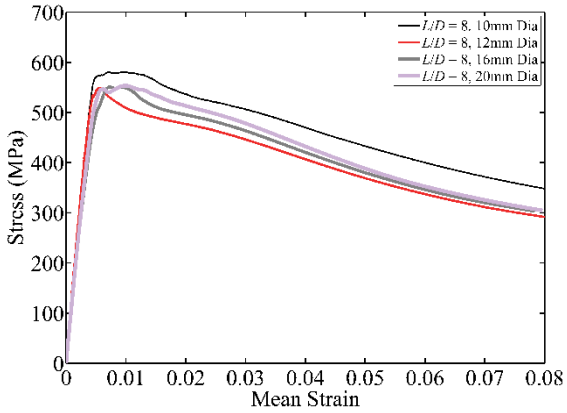

(b)

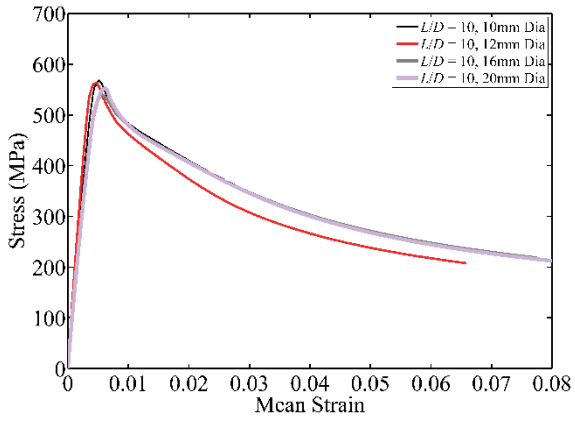

(c)

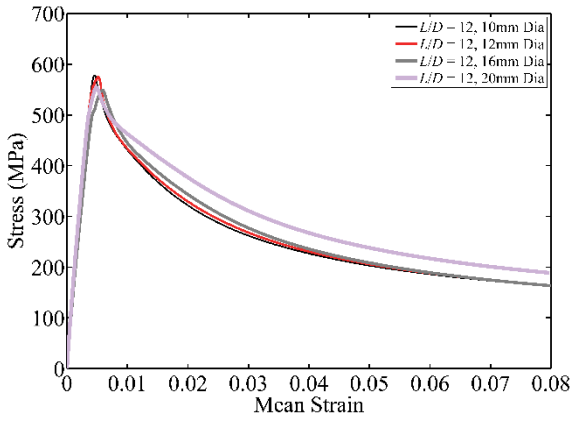

(d)

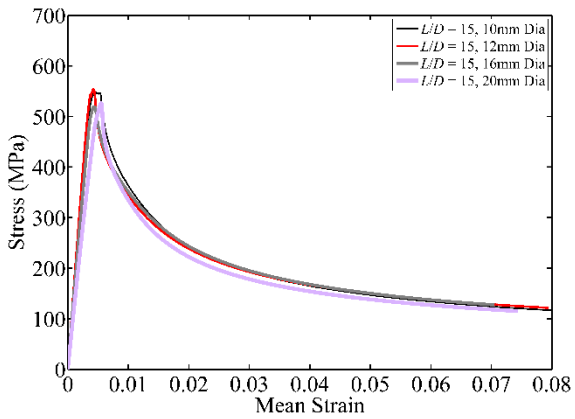

(e)

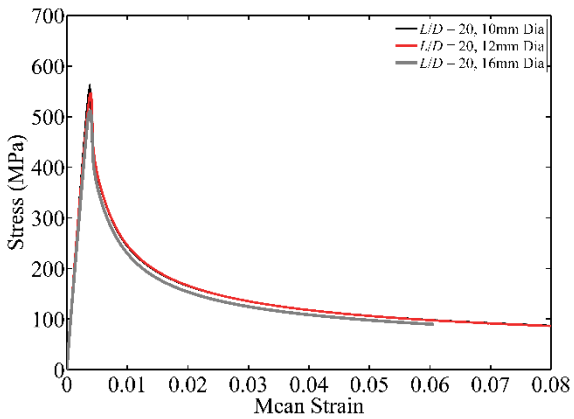

(f)

Fig. 4 Nonlinear buckling response of uncorroded reinforcing bars: (a) *L*/*D* = 5, (a) *L*/*D* = 8, (a) *L*/*D* = 10, (a) *L*/*D* = 12, (a) *L*/*D* = 15, (a) *L*/*D* = 20

3.3 Monotonic buckling test of corroded bars

A total of 86 buckling tests on corroded specimens were conducted. The *L/D* ratios used in buckling tests of corroded bars are 5, 10 and 15. Examples of buckled bars with various *L/D* ratios and mass losses are shown in Fig. 5. The detailed results are discussed in the following sections 3.3.1 to 3.3.5 of this paper.

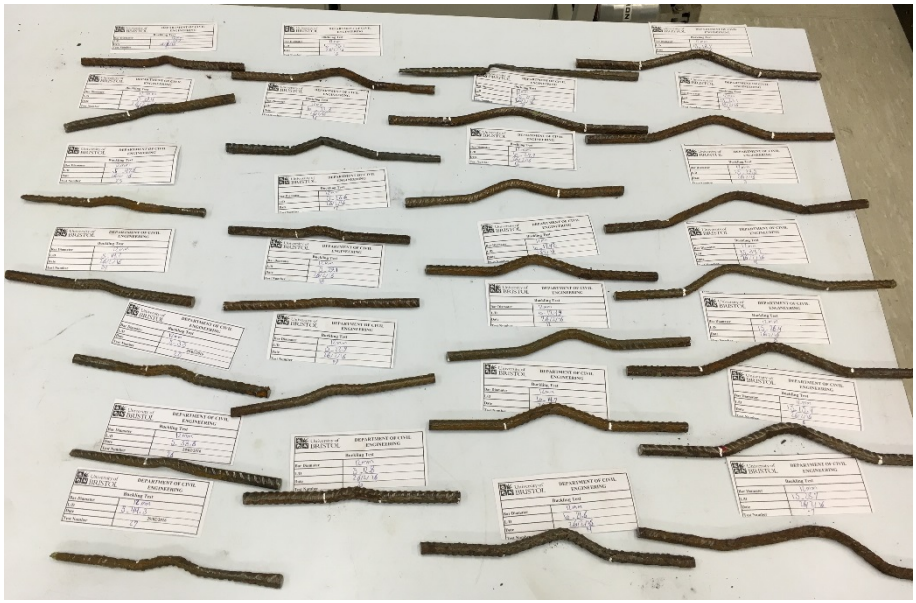

Fig. 5 Examples of 12mm diameter corroded bars with various mass losses and slenderness ratios after buckling tests

3.3.1 *Influence of bar diameter on post-yield buckling behaviour of corroded bars with L/D = 5*

Fig. 6 shows the average stress-strain response of corroded reinforcing bars with *L*/*D* = 5. The response of corresponding uncorroded control specimens are also included in Fig. 6 to be compared with the corroded specimens. As explained in the previous section, the stress-strain response of uncorroded bars with *L*/*D* = 5 is almost identical to the stress-strain response in tension. This is because the buckling length of uncorroded bars with *L*/*D* = 5 is very small. Therefore, after buckling the significant portion of the length of the bar becomes plastic.

Moreover, the lateral deformation due to buckling is very small and the geometrical nonlinearity (second order effect) is almost negligible. However, corrosion resulted in a reduction in yield stress (mean stress based on mean reduced area) in these bars and subsequently premature buckling. For most bars the post-yield behaviour followed the same pattern as tension envelope. Only, a few highly corroded specimens with percentage mass loss of more than about 40% showed some softening type response due to buckling. For example a 20mm diameter bar with 56.23% mass loss ratio shown in Fig. 6(d) has severe post-yield softening response. This is because corrosion changes the effective slenderness ratio of corroded specimens. The buckled shaped of this corroded bar is shown in Fig. 7(a) and compared with another bar with 16mm diameter and 22.1% mass loss ratio. Fig. 5 shows that bar diameter does not generally change the post-yield buckling response of corroded bars unless there is a severe localised corrosion similar to the corroded bar shown in Fig. 7(a). It was found that bar diameter does not have any influence on the shape of the stress-strain response of corroded bars in post-yield region. Therefore, we can conclude that bar dimeter does not have a significant influence on post-yield response of corroded bars with L/D = 5. The influence of bar diameter on yield stress of this group of bars is investigated in sections 3.3.4 and 3.3.5 of this paper.

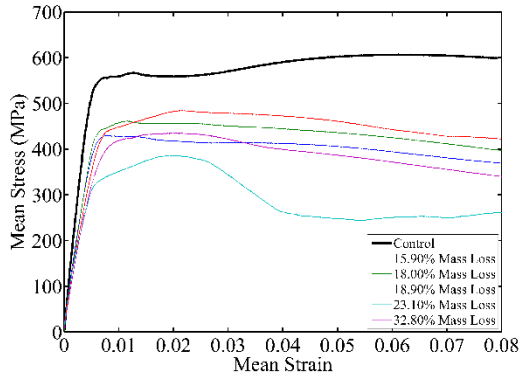

(a)

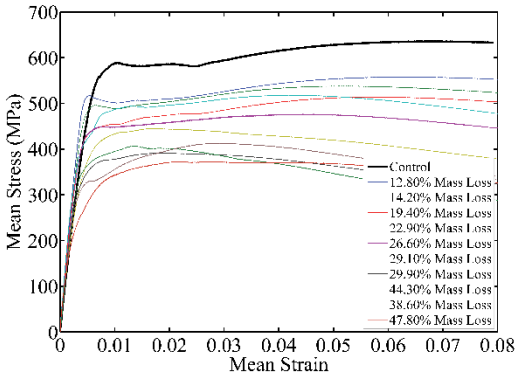

(b)

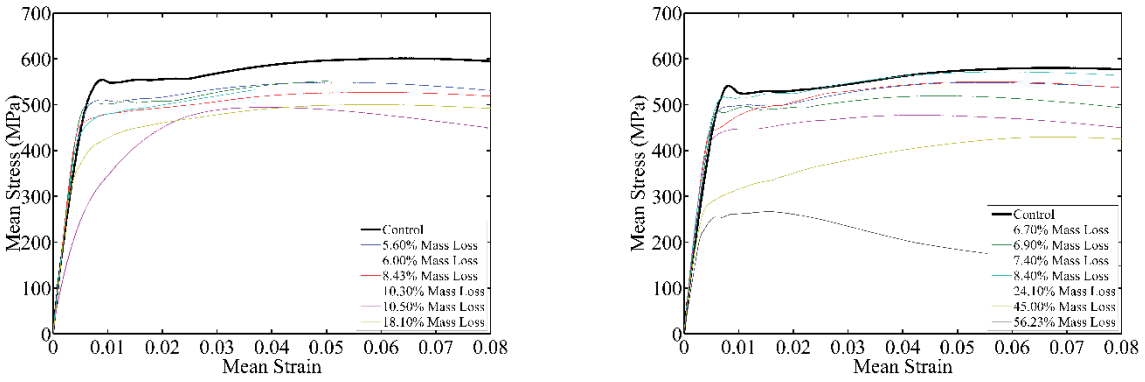

(c) **(d)**

Fig. 6 Nonlinear buckling response of corroded reinforcing bars with *L*/*D* = 5: (a) 10mm diameter bars, (b) 12mm diameter bars and (c) 16mm diameter bars and (d) 20mm diameter bars

(a)

(b)

Fig. 7 Examples of buckled corroded reinforcing bars with *L*/*D* = 5: (a) 20mm diameter bar and (b) 16mm diameter bar

3.3.2 *Influence of bar diameter on post-yield buckling behaviour of corroded bars with L/D = 10*

Fig. 8 shows the average stress-strain response of corroded bars with L/D = 10. The uncorroded control specimens in this group of bars had a stable behaviour up to yield stress. They then showed a softening type response in post-yield buckling region. The bars with highly localised pitting corrosion showed a small yield plateau after yielding and subsequently a post-yield softening (e.g. Fig. 8 (a) 22.13% mass loss). This is due to the yielding and squashing of the smallest pitted section prior to buckling. This behaviour was consistent in all bar diameters. The post-yield buckling response of this group of corroded bars with different bar dimeter showed a similar trend to their corresponding uncorroded

specimens but with a reduction in the buckling stress. Fig. 8 shows that as the bar diameter increases some differences in the post-yield buckling response of corroded bars are seen. It shows that corroded bars with bigger diameter (16mm and 20mm compare to 10mm and 12mm) start yielding and subsequently buckling earlier than bars with smaller diameter. This is due to the influence of pitting corrosion induced imperfection along the length of corroded bars. This shows that the impact of imperfection increases in corroded bars as bar diameter increases and is quantified through regression analysis of experimental data in sections 3.3.4 and 3.3.5 of this paper.

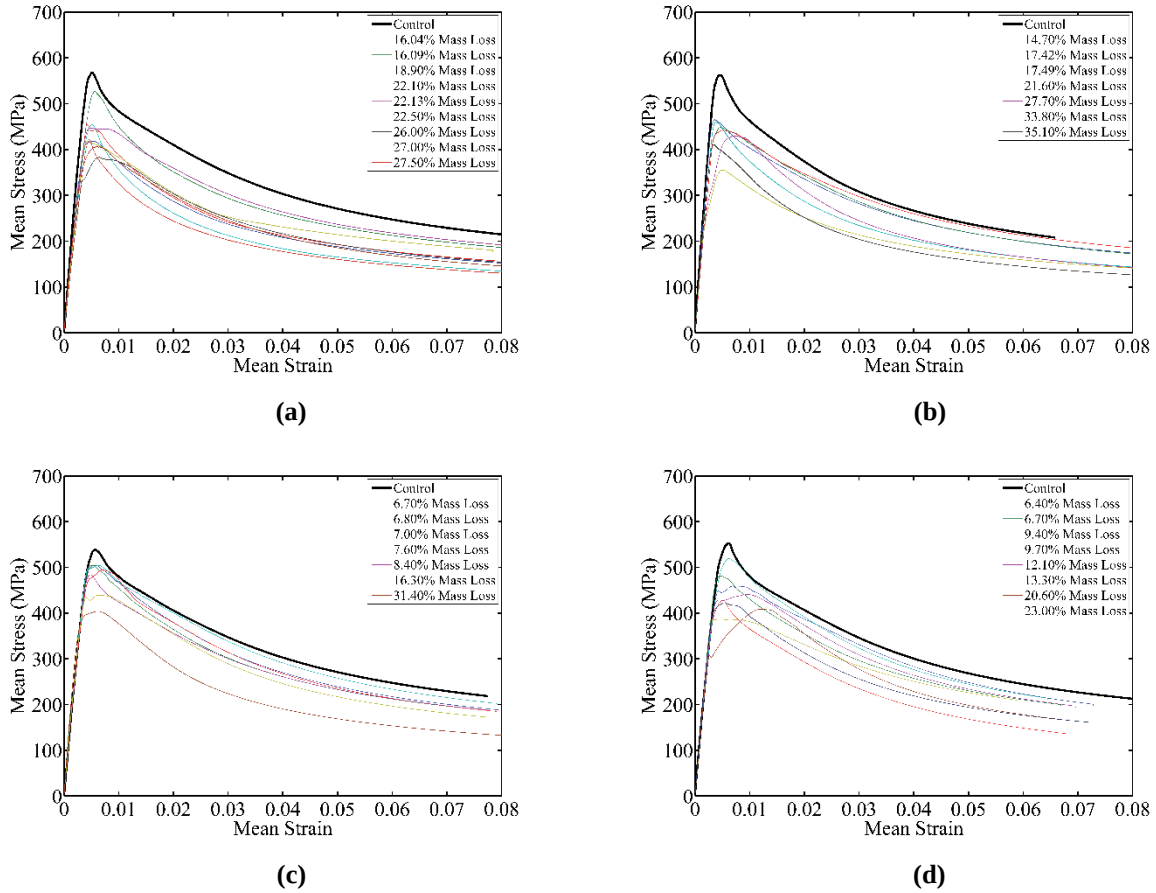

Fig. 8 Nonlinear buckling response of corroded reinforcing bars with L/D = 10: (a) 10mm diameter bars, (b) 12mm diameter bars and (c) 16mm diameter bars and (d) 20mm diameter bars

3.3.3 *Influence of bar diameter on post-yield buckling behaviour of corroded bars with L/D = 15*

Fig. 9 shows the average stress-strain response of corroded bars with L/D = 15. The uncorroded specimens for this group of bars in all diameters showed a stable behaviour up to yield stress and then a sharp and steep post-yield buckling response was observed. All the corroded bars with L/D = 15 generally showed a sharp transition from linear elastic to post-yield softening compared to corroded bars with L/D = 5 and 10. This is due to the more severe impact of geometric nonlinearity on the post-yield buckling response. It is also observed that the corroded bars with L/D = 15 yield and subsequently buckle earlier than the group of bars with L/D = 10. This is quantified in sections 3.3.4 and 3.3.5 of this paper.

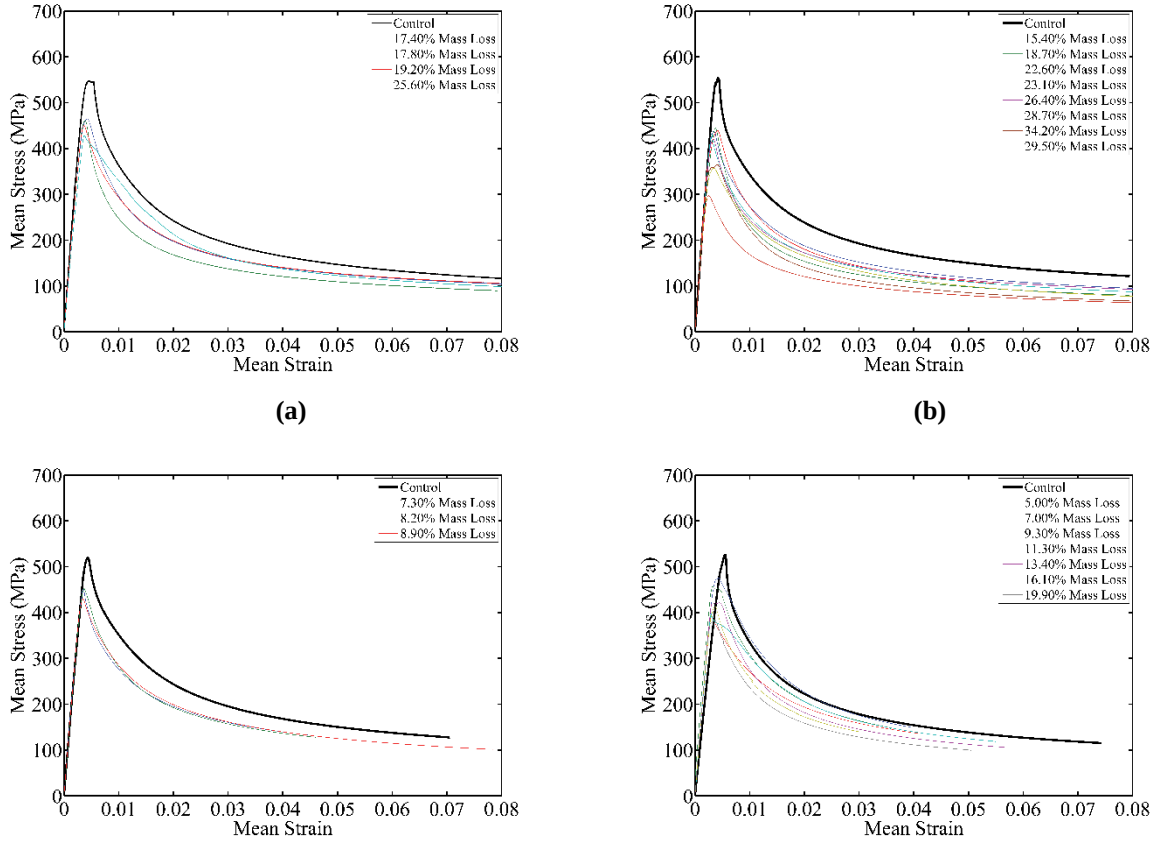

Fig. 9 Nonlinear buckling response of corroded reinforcing bars with L/D = 15: (a) 10mm diameter bars, (b) 12mm diameter bars and (c) 16mm diameter bars and (d) 20mm diameter bars

3.3.4 *Influence of corrosion on buckling stress reduction of reinforcing bars*

The impact of corrosion on the buckling stress reduction (buckling capacity reduction) of corroded bars is investigated by linear regression analysis. In the regression analysis of corroded bars with L/D = 5, the ratio of mean yield compressive stress of corroded specimens to the corresponding values in uncorroded specimens used. This is because the onset of buckling in the group of bars with L/D = 5 is not clear from the experimental data. However, the buckling occurs after yielding of reinforcement. Therefore, the yielding point of bars in compression is the most important factor affecting the buckling capacity of bars in compression. In the group of bars with L/D = 10 and 15 the onset of buckling was clear from the experimental data. Therefore, the ratio of mean maximum compressive stress (stress at onset of buckling) of corroded specimens to the corresponding values of maximum compressive stress of uncorroded bars used for the group of bars with L/D = 10 and 15. Fig. 10 shows the results of the linear regression analyses of the group of bars with L/D = 5 and Fig. 11 shows the results of the linear regression analyses of the group of bars with L/D = 10 and 15. The equation of the best fit line to the experimental data (shown in Fig. 10 and 11) is defined in Eq. (1).

$$\sigma'_{yc} = \sigma_{yc}(1-\alpha\ \psi) \tag{1}$$

where, σ'_{yc} is the buckling stress of corroded bar, σ_{yc} is the buckling stress of uncorroded bar, α is buckling stress pitting coefficient and ψ is percentage mass loss. The values of buckling stress pitting coefficient (α) are summarised in Table 2. The calculated pitting coefficients are in good agreement with the experimental results obtained by Kashani et al. (2013a). However, the experimental study conducted by Kashani et al (2013a) was only limited to 12mm diameter bars. The influence of bar diameter (size effect) on buckling stress pitting coefficient is discussed in the section 3.3.5 of this paper.

Table 2 Buckling stress pitting coefficients (α)

Bar Diameter	10	12	16	20
L/D = 5	0.012	0.01321	0.01904	0.01816
L/D = 10 and 15	0.00909	0.00943	0.01043	0.01442

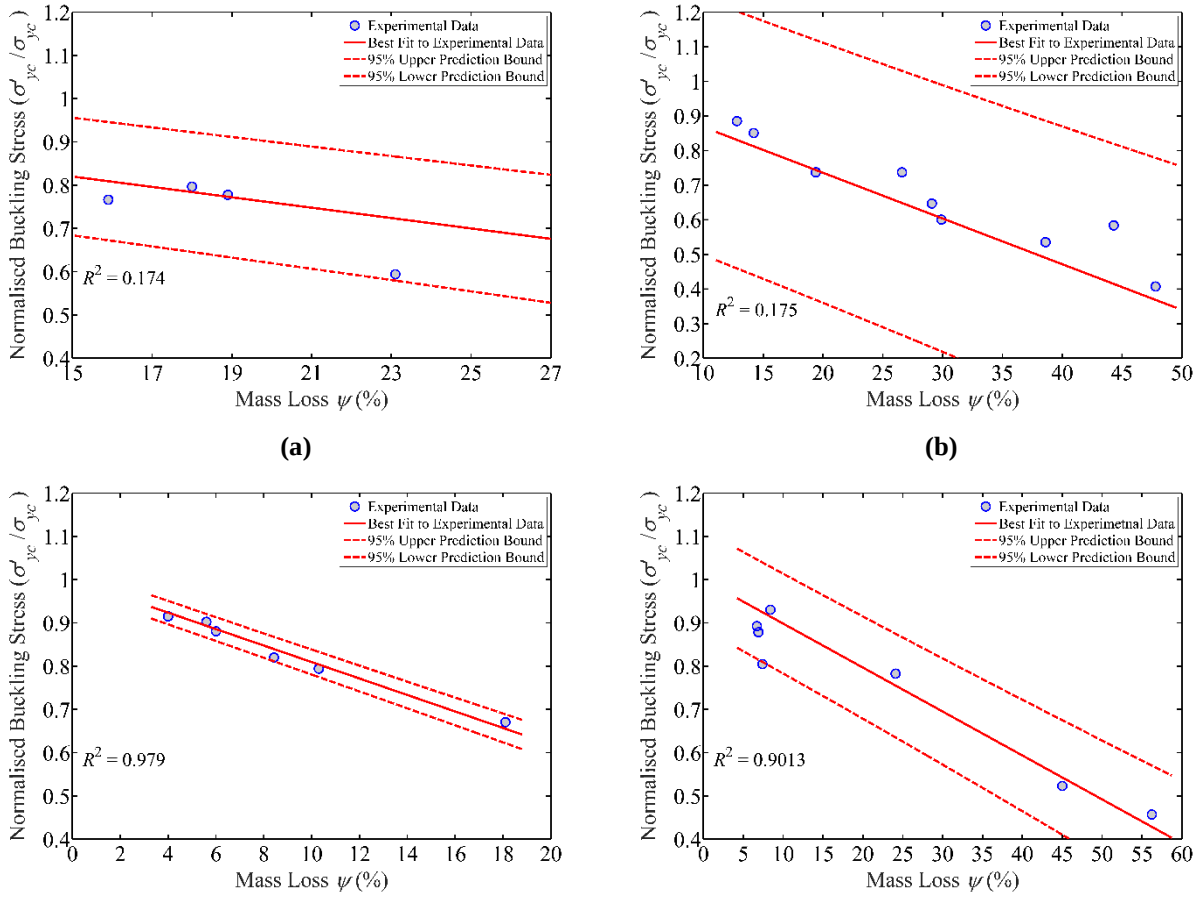

Fig. 10 Influence of corrosion on buckling stress of reinforcing bars with *L/D* = 5: (a) 10mm diameter bars, (b) 12mm diameter bars and (c) 16mm diameter bars and (d) 20mm diameter bars

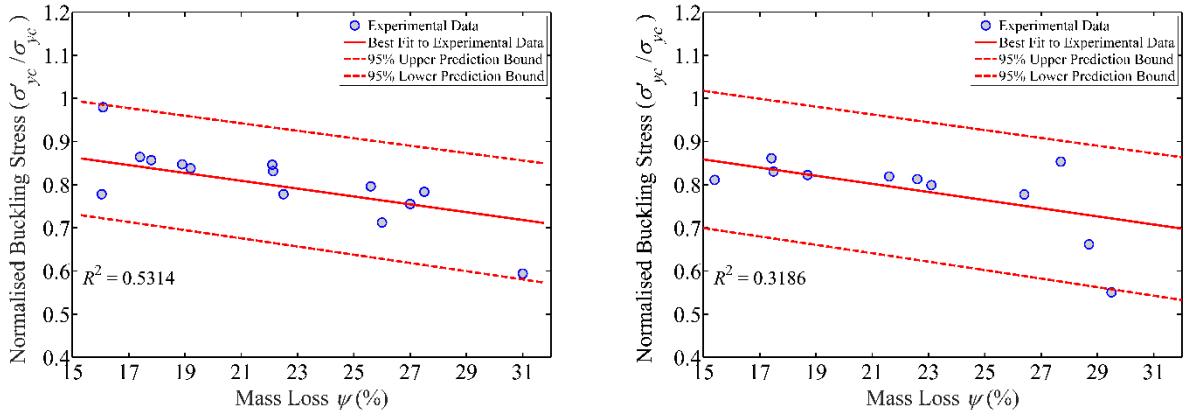

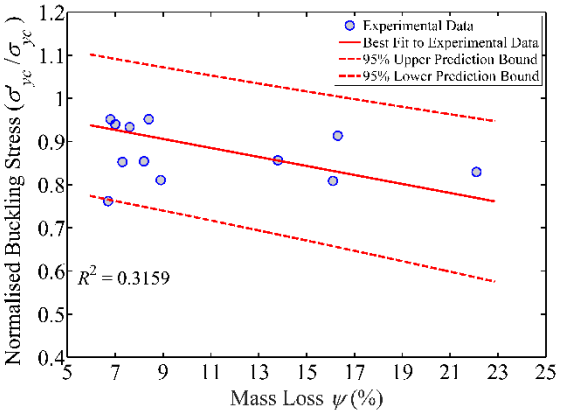

(c)

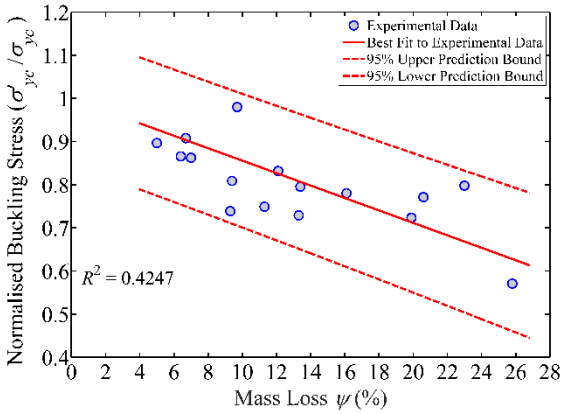

(d)

Fig. 11 Influence of corrosion on buckling stress of reinforcing bars with *L*/*D* = 10 and 15: (a) 10mm diameter bars, (b) 12mm diameter bars and (c) 16mm diameter bars and (d) 20mm diameter bars

3.3.5 *Correlation between buckling stress pitting coefficient and bar diameter*

The correlation between the pitting coefficients (reported in Table 1) and bar diameter is investigated through nonlinear regression analysis. Fig. 12 shows the results of these regression analyses. The equations of the best fit lines are described in Eqs. (2) and (3). The results of regression analyses show that there is a strong positive correlation between bar diameter and pitting coefficient. This shows that as the bar diameter increases the impact of corrosion on buckling capacity increases. This is due to the influence of non-uniform pitting corrosion along the length of corroded bars. The non-uniform pitting corrosion induces imperfections along the length of the bar. Therefore, as the bar diameter increases the impact of imperfection on buckling capacity of corroded bars increases. This is a very important finding that is crucial in modelling the nonlinear behaviour of corroded RC structures.

$$\alpha = 0.0029\ x^{0.628} \tag{2}$$

$$\alpha = 0.005\ \exp(0.049\,x) \tag{3}$$

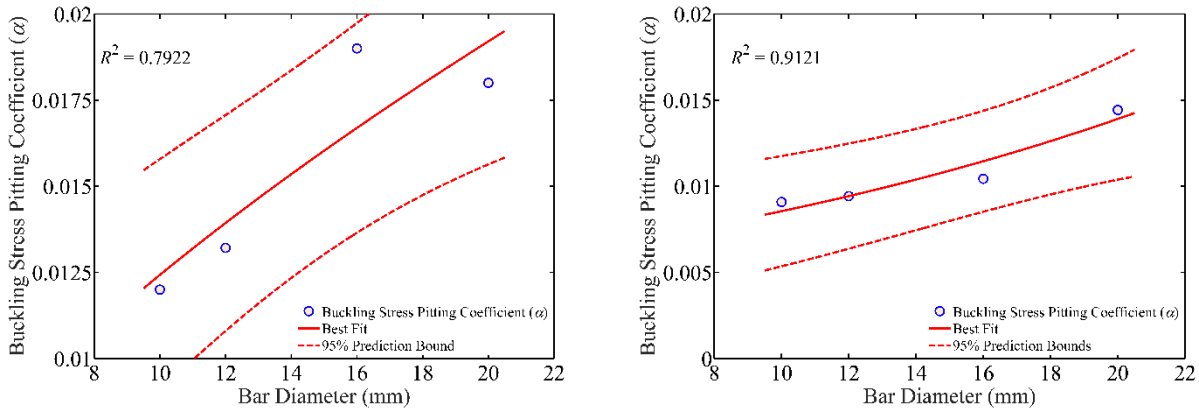

(a) **(b)**

Fig. 12 Size effect on buckling stress pitting coefficient of corroded bars: (a) group of bars with *L*/*D* = 5 and (b) group of bars with *L*/*D* = 10 and 15

It should be noted that the outcome of the regression analysis in this section is based on limited experimental data. There is need for further experimental testing on a wider range of bar diameters and yields strengths. Nevertheless, the research reported in paper highlighted this important issue to other researchers for future research.

4. Critical review and comparison of the observed experimental results with state-of-the-art computational and analytical models

4.1 Nonlinear micro-fibre finite element analysis of uncorroded bars

Previous research (Dhakal and Maekawa 2002; Kashani et al. 2014) showed that fibre-based finite element models are able to accurately model material and geometrical nonlinearity in nonlinear buckling analysis of reinforcing bars. Dahakal and Maekawa (2002) and Kashani et al. (2014) mployed this technique to develop a uniaxial material model for reinforcing bars accounting for inelastic buckling to be used in nonlinear analysis of RC structures. However, in both studies the influence of bar diameter on the results of finite element analyses was not investigated. Therefore, in this section a set of nonlinear buckling analyses are conducted for bars with different diameters to investigate if the bar diameter influences the accuracy of nonlinear analysis results. It should be noted that only uncorroded specimens are considered in this section.

OpenSees, an open-source three-dimensional nonlinear finite element code is employed. A force-based distributed plasticity nonlinear fibre beam-column element available in the OpenSees is used (Spacone et al. 1996a,b). This element formulation assumes a linear moment distribution and constant axial force distribution along the length of the element. Nonlinear material response under flexural-type loading is simulated at the section level using fibre-based section discretisation technique. Each fibre response is defined using a nonlinear constitutive model. The moment and axial force at section level are determined by integrating the fibre stresses over the cross section. The generalised nodal displacements are then determined from section deformations using a Gauss-Labotto integration scheme. To model geometrical nonlinearity and second order effect due to buckling, co-rotational transformation available in the OpenSees is used (Neuenhofer and Filippou 1998). An initial imperfection of 0.001mm (1.0×10^{-5} to 4.16×10^{-6} of L where L is the length of the bar) was introduced at mid height of the bar to initiate buckling (the initial imperfect shape was linear). To emulate the boundary conditions during the laboratory tests, the rotations and displacements of the bottom node of the bars were fully restrained in the model. The axial displacement history applied in the laboratory experiments was applied in the analyses. Further details of the finite element model development, the nonlinear uniaxial material model used in the analyses and model verification are available in (Kashani et al. 2014).

Fig. 13(a) and (b) shows the results of inelastic buckling analyses of reinforcing bars with 10mm and 20mm bar diameter and $L/D = 5$. The results show that the fibre model is not able to accurately simulate the post-yield buckling response of these groups of bars. As explained in section 3.2 the spread of plasticity almost covers the whole length of short bars ($L/D \leq 8$). Therefore, the 3D effect of material plasticity and subsequently size effect is more significant. The fibre model employs uniaxial material models and in the presence of severe

3D material plasticity it is unable to predict the combined effect of material and geometrical nonlinearity.

Fig. 13(c) and (d) shows the results of inelastic buckling analyses of reinforcing bars with 10mm and 20mm bar diameter and L/D = 15. The analysis results show that, in this case, nonlinear micro-fibre analysis can capture the inelastic buckling and post buckling behaviour of reinforcing bars with different diameters. This is because the material plasticity in bars with larger slenderness ratio (L/D > 8) is localised in plastic hinge locations. Therefore, the 3D effect of material plasticity and size effect is less significant. In these cases (L/D > 8) fibre model can accurately simulate the post-yield buckling response of reinforcing bars. Therefore, it can be concluded that the impact of size effect (influence of bar diameter) on post-yield buckling response of reinforcing bar is a function of slenderness ratio.

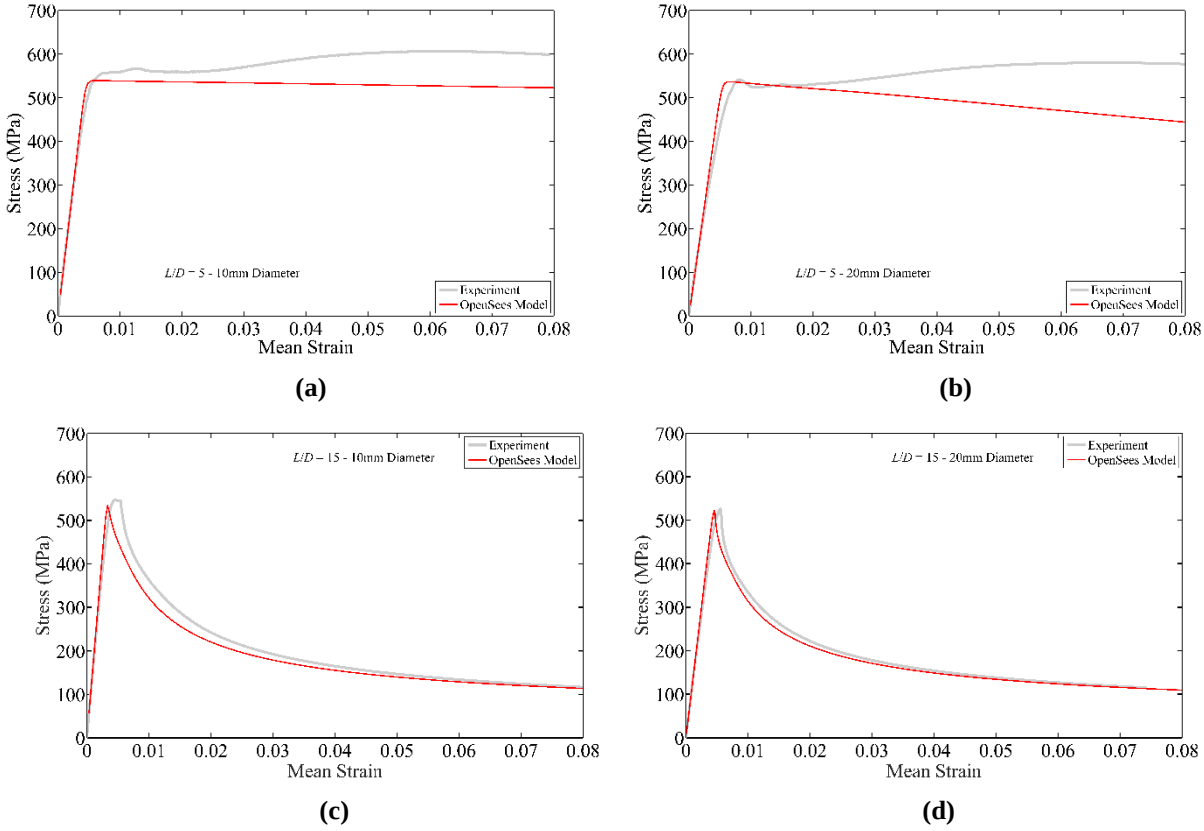

Fig. 13 Comparison of the experimental results of uncorroded bars with OpenSees simulations: (a) 10mm diameter, (b) 12mm diameter, (c) 16mm diameter and (d) 20mm diameter

4.2 Comparison of experimental results with Kashani's uniaxial material model to simulate the post-yield buckling behaviour of uncorroded and corroded bars

Kashani et al. (2015b) developed a new phenomenological uniaxial material model to simulate the inelastic buckling and post-yield buckling behaviour of corroded and uncorroded reinforcing bars. Kashani's model calibrated against a comprehensive set of experimental data of uncorroded and corroded reinforcing bars. This model is also able to simulate the nonlinear cyclic behaviour of uncorroded and corroded bars with the effect of inelastic buckling and low-cycle fatigue degradation. In this model, the post-yield buckling response of reinforcing bars is a function of a compound slenderness ratio known as λ_p [Eq. (4)].

$$\lambda_p = \sqrt{\frac{\sigma_y}{100}}\frac{L}{D} \tag{4}$$

where, σ_y is the yield strength of reinforcing bars in tension. The λ_p initially proposed by Dhakal and Maekawa (2002) which then employed by Kashani et al. (2015b) in their model. Further details are available in Kashani et al. (2015b). Eq. (4) shows that the post-yield buckling response of reinforcing bars in the analytical model is independent from bar diameter. Therefore, the model does not account for the influence of bar diameter on post-yield buckling response of reinforcing bars. Moreover, this model is developed and calibrated using the experimental data of uncorroded and corroded 12mm diameter bars and has not been validated and verified for post-yield buckling simulation of uncorroded and corroded bars with different bar diameters. In this section, a comparison between the experimental results and Kashani's phenomenological model is made. Fig. 14 shows an example comparison of the experimental results of uncorroded bars with the Kashani's model. The comparison of results show that although the analytical model is independent from the bar diameter it is still able to accurately simulate the post-yield buckling response of uncorroded reinforcing bars.

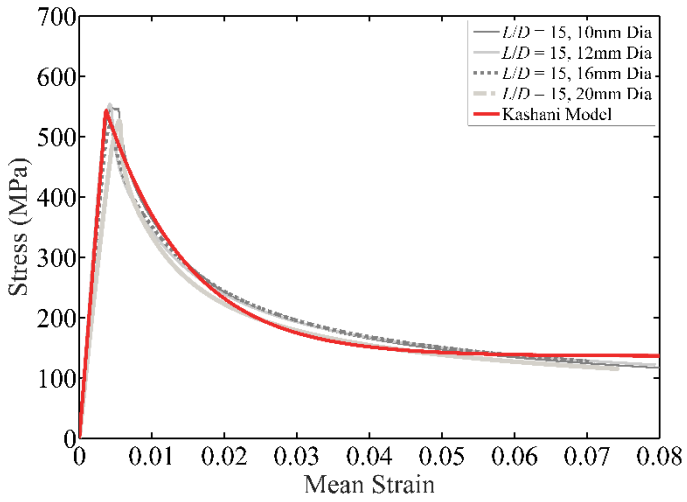

Fig. 14 Comparison of the experimental results of uncorroded bars with Kashani uniaxial material model

Furthermore, the results of regression analyses are used [Eq. (3)] to update this model to account for influence of bar diameter on buckling stress reduction of corroded bars. Fig. 15 (a-d) shows a comparison between the Kashani's updated model and the observed experimental results. Comparison of results shows that the updated model can accurately simulate the inelastic buckling response of corroded reinforcing bars accounting for the influence of bar diameter. As mentioned previously, there is still need for further experimental studies for further verification and calibration of these models in the future research. However, the model developed by Kashani et al. (2015b) is currently the only model available in the literature which is able to simulate the nonlinear stress-strain behaviour of corroded bars accounting for bar buckling effect. This model is implemented in the OpenSees and is readily available to the community to be used in nonlinear analysis of RC structures and bridges.

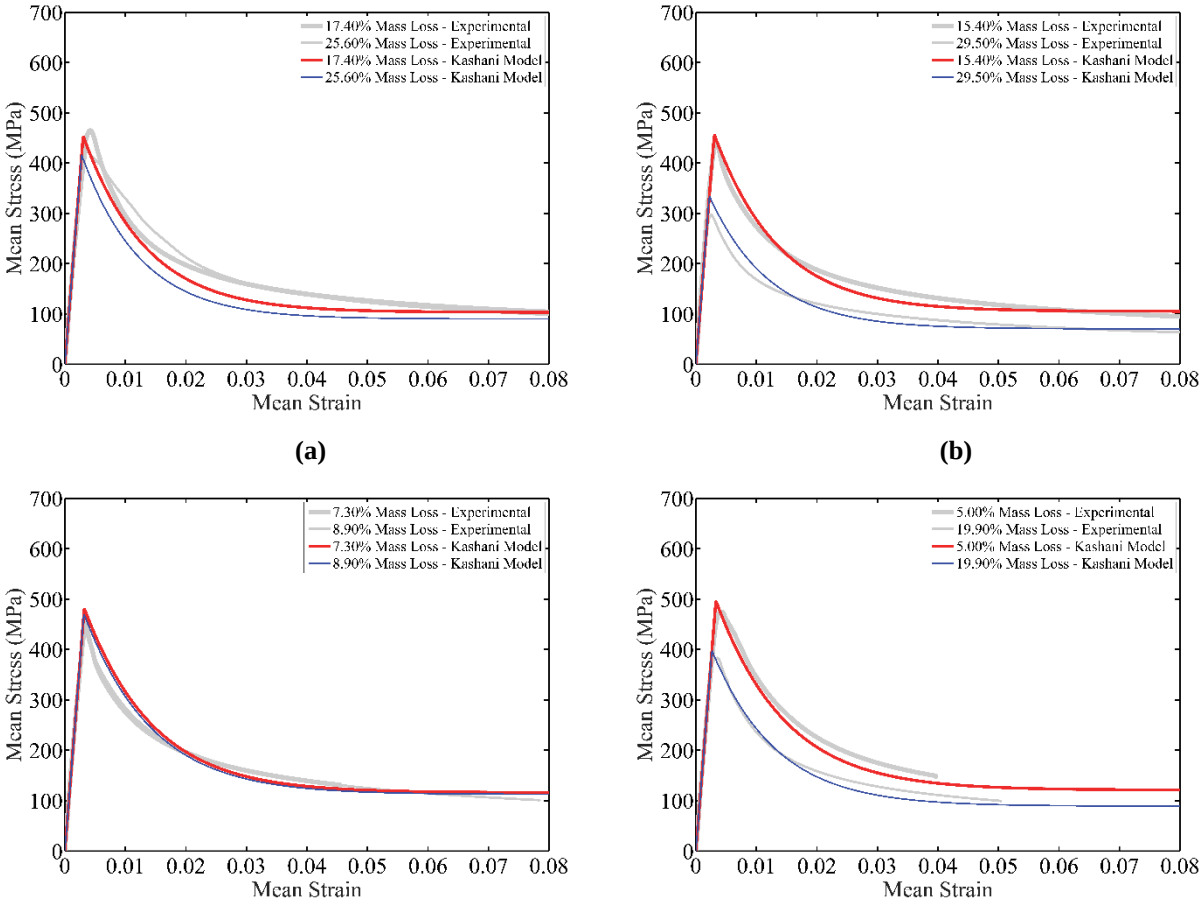

Fig. 15 Comparison of the experimental results of corroded bars with Kashani uniaxial material model: (a) 10mm diameter, (b) 12mm diameter, (c) 16mm diameter and (d) 20mm diameter

5. Conclusion

A total of 24 buckling tests on uncorroded bars and 86 buckling tests on corroded bars varied in slenderness ratios and bar diameters are conducted. Influence of bar diameter on buckling and post-yield buckling response of uncorroded bars is investigated. Combined influence of corrosion and bar diameter on buckling stress reduction of corroded bars is explored using regression analysis of experimental data. The key findings of this research can be summarised as follows:

(1) The comparison of buckling tests on uncorroded bars with different bar diameters showed that the size effect is more significant in bars with $L/D \leq 8$. This is due to the impact of material plasticity in these bars. Further computational research using 3D

continuum finite element analysis is required to investigate this phenomenon in more detail. However, in structural engineering point of view, the influence of bar diameter on inelastic buckling behaviour of bars is negligible as it will not have any significant impact on flexural capacity and inelastic behaviour of RC sections/components.

(2) The influence of corrosion on buckling stress reduction of reinforcing bars is investigated using linear regression analysis of experimental data. The calculated pitting coefficient of buckling stress reduction is in good agreement with the results observed by Kashani (2013a).

(3) The comparison of results show that bar diameter has a considerable influence on the buckling stress reduction of corroded bars. This is investigated through nonlinear regression analysis of pitting coefficients for bars with different diameters. The analyses results show that there is a strong positive correlation between buckling stress pitting coefficient and bar diameter. In other words, as the bar diameter increases the pitting coefficient increases (i.e. reduction in buckling capacity increases). This is because the non-uniform pitting corrosion induces imperfections along the length of corroded bars. These results show that the impact of corrosion induced imperfection increases as bar diameter increases.

(4) Although the experimental results of this research show that bar diameter has an impact on buckling capacity loss (buckling stress reduction) of corroded bars, there is still need for further experimental testing on corroded bars with wider range of bar diameters and mechanical properties. Nevertheless, the outcome of this research highlights that the size effect has a considerable impact on buckling capacity loss of corroded bars and is an important area for future research. Moreover, there is a need for a similar study on corroded bars in tension to explore the significance of size effect on mechanical properties and ductility loss of corroded bars in tension.

(5) Comparison of the experimental results reported in this paper with Kashani's phenomenological model (Kashani 2015b) showed that this model can accurately simulate the post-yield buckling behaviour of uncorroded and corroded reinforcing bars. This model is implemented in the OpenSees and is readily available to the community (researchers and practicing engineers) to be used in nonlinear analysis of corroded RC structures.

Acknowledgement

The author would like to thank Mr Mehdi Bozorg for conducting the experimental testing of this research as part of his 3rd year undergraduate research project at the University of Bristol laboratories.

References

ASTM G1-03 Standard Practice for preparing, cleaning, and evaluating corrosion test specimens, ASTM Int'l 2011.

Akiyama M, Frangopol DM and Matsuzaki H. Life-cycle reliability of RC bridge piers under seismic and airborne chloride hazards. Earthq Eng Struct D, (2011) 40: 1671–1687.

Alipour A, Shafei B and Shinozuka M. Performance evaluation of deteriorating highway bridges located in high seismic areas. J Bridge Eng, (2011) 6 (5): 597-611.

Almusallam AA. Effect of degree of corrosion on the properties of reinforcing steel bars. Const and Build Mat, (2001) 15: 361-368.

Apostolopoulos CA, Papadopoulos MP, Pantelakis SG. Tensile behavior of corroded reinforcing steel bars BSt 500s. Construct and Build Mater, (2006) 20: 782–789.

Apostolopoulos CA. Mechanical behavior of corroded reinforcing steel bars S500s tempcore under low cycle fatigue. Construct and Build Mater (2007) 21: 1447–1456.

Bae S, Mieses A, Bayrak O. Inelastic buckling of reinforcing bars. J of Struct Eng, (2005) 131 (2): 314–321.

Bayrak O and Sheikh SA. Plastic hinge analysis. J of Struct Eng, (2001) 127(9): 1092–1100.

Berry M, Eberhard MO. Performance Models for Flexural Damage in Reinforced Concrete Columns. Berkeley: Pacific Earthquake Engineering Research Centre (2003).

BS 4449-2005 +A2. Steel for the reinforcement of concrete - Weldable reinforcing steel - bar, coil and decoiled product – Specification; 2009.

Bresler B and Gilbert PH. The requirements for reinforced concrete columns. ACI J, (1961) 58 (5) 555–570.

Cosenza E, and Prota A. Experimental behavior and numerical modeling of smooth steel bars under compression, J of Earthquake Eng (2006) 10(3): 313-329.

Cairns J, Plizzari GA, Du YG, Law DW, and Chiara F. Mechanical properties of corrosion-damaged reinforcement. ACI Mat J, (2005) 102 (4): 256–264.

Dhakal RP, Maekawa K. Modeling for postyield buckling of reinforcement. J of Struct Eng, (2002) 128 (9): 1139–1147.

Du YG, Clark LA, Chan AHC. Residual capacity of corroded reinforcing bars. Magazine of Conc Res, (2005) 57 (3): 135–147.

Du YG, Clark LA, Chan AHC. Effect of corrosion on ductility of reinforcing bars. Magazine of Conc Res, (2005) 57 (7): 407–419.

Gomes A, Appleton J. Nonlinear cyclic stress-strain relationship of reinforcing bars including buckling. Eng Struct, (1997) 19: 822–826.

Ghosh J and Padgett JE. Aging considerations in the development of time-dependent seismic fragility curves. J Struct Eng, (2010) 136 (12): 1497–1511.

Kashani MM. Seismic Performance of Corroded RC Bridge Piers: Development of a Multi-Mechanical Nonlinear Fibre Beam-Column Model. PhD Thesis, Bristol: University of Bristol (2014).

Kashani MM, Crewe AJ, Alexander NA. Nonlinear stress-strain behaviour of corrosion-damaged reinforcing bars including inelastic buckling. Eng Struct, (2013a) 48: 417–429.

Kashani MM, Crewe AJ, Alexander NA. Nonlinear cyclic response of corrosion- damaged reinforcing bar with the effect of buckling. Constr Build Mater, (2013b) 41 388–400.

Kashani MM, Lowes LN, Crewe AJ, Alexander NA. Finite element investigation of the influence of corrosion pattern on inelastic buckling and cyclic response of corroded reinforcing bars. Eng Struct, (2014) 75: 113-125.

Kashani, M.M., Alagheband, P., Khan, R., & Davis, S. Impact of corrosion on low-cycle fatigue degradation of reinforcing bars with the effect of inelastic buckling. International Journal of Fatigue, (2015a) 77: 174-185.

Kashani MM, Lowes LN, Crewe AJ, Alexander NA. Phenomenological hysteretic model for corroded reinforcing bars including inelastic buckling and low-cycle fatigue degradation. Comput Struct, (2015b) 156: 58-71.

Kashani MM, Barmi AK, Malinova VS. Influence of inelastic buckling on low-cycle fatigue degradation of reinforcing bars. Constr Build Mater, (2015c) 644-655.

Kashani MM, Lowes LN, Crewe AJ, Alexander NA. Nonlinear fibre element modelling of RC bridge piers considering inelastic buckling of reinforcement. Eng Struct, (2016a) 116: 163-177.

Kashani MM, Lowes, L. N., A., Crewe, A. J., Alexander, N. A multi-mechanical nonlinear fibre beam-column model for corroded columns, International Journal of Structural Integrity, (2016b) 7(2): 213 - 226.

Kunnath SK, Heo Y and Mohle JF. Nonlinear uniaxial material model for reinforcing steel bars. J Struct Eng, (2009) 135 (4): 335-343.

Lehman DE, Moehle JP. Seismic performance of well-confined concrete bridge columns. Berkeley: Pacific Earthquake Engineering Research Centre, (2000).

Ma Y, Che Y and Gong J. Behavior of corrosion damaged circular reinforced concrete columns under cyclic loading. Constr Build Mater, (2012) 29: 548–556.

Mau ST. Effect of tie spacing on inelastic buckling of reinforcing bars. ACI Struct J, (1990) 87 (6): 671–678.

Mau ST, El-Mabsout M. Inelastic buckling of reinforcing bars. J of Eng Mech, (1989) 115 (1): 1–17.

Meda A, Mostosi S, Rinaldi Z, Riva P. Experimental evaluation of the corrosion influence on the cyclic behaviour of RC columns. Eng Struct, (2014)76:112–23.

Monti G, Nuti C. Nonlinear cyclic behavior of reinforcing bars including buckling. J of Struct Eng, (1992) 118 (12): 3268–3284.

Ni Choine M., Kashani M.M., Lowes L.N., O'Connor A., Crewe A.J., Alexander N.A., & Padgett J.E. Nonlinear dynamic analysis and seismic fragility assessment of a corrosion damaged integral bridge. International Journal of Structural Integrity, (2016) 7(2): 227 - 239.

Neuenhofer A, Filippou FC. Geometrically nonlinear flexibility-based frame finite element, J Struct Eng, (1998) 124 (6): 704-711.

OpenSees, the Open System for Earthquake Engineering Simulation, PEER (2016), University of California, Berkeley.

567 Ou Y, Tsai L and Chen H. Cyclic performance of large-scale corroded reinforced concrete
568 beams. Earthq Eng Struct D, (2011) 41: 592-603.

569 Palssom, R, Mirza MS. Mechanical response of corroded steel reinforcement of abandoned
570 concrete bridge. ACI Struct J, (2002) 99(2): 157–162.

571 Pantazopoulou SJ. Detailing for reinforcement stability in reinforced concrete members. J of
572 Struct Eng, (1998) 124(6): 623–632.

573 Papia M, Russo G. Compressive concrete strain at buckling of longitudinal reinforcement. J
574 of Struct Eng, (1989) 115(2): 382–397.

575 Restrepo-Posada J, Dodd L, Park R and Cooke N. Variables effecting cyclic behavior of
576 reinforcing steel. J of Struct Eng, (1994) 120 (11), 3178–3196.

577 Rodriguez ME, Botero JC, Villa J. Cyclic stress-strain behavior of reinforcing steel including
578 the effect of buckling. J of Struct Eng, (1999) 125 (6): 605–612.

579 Spacone, E., Filippou, F.C. & Taucer, F.F. Fibre beam-column model for non-linear analysis
580 of R/C frames: part I: formulation. Earthquake Engineering and Structural Dynamics, (1996)
581 25: 711-725.

582 Spacone, E., Filippou, F.C. & Taucer, F.F. Fibre beam-column model for non-linear analysis
583 of R/C frames: part II: applications. Earthquake Engineering and Structural Dynamics, (1996)
584 25: 727-742.

585 The economic impact of current investment trends in surface transportation infrastructure.
586 Economic Development Research Group Inc: ASCE, 2011.